INTERNATIONAL JOURNAL OF HYDROGEN ENERGY 36 (2011) 9037–9044

Available at www.sciencedirect.com

ScienceDirect

journal homepage: www.elsevier.com/locate/he

Interaction of hydrogen and platinum over a B2 FeTi (110) Slab

J.M. Marchetti [a,b,*], E. González [b], P. Jasen [b], G. Brizuela [b], A. Juan [b]

[a] Chemical Engineering Department, Faculty of Natural Science and Technology, Sem Sælands v. 4, 7491 Trondheim, Norway
[b] Departamento de Física, Universidad Nacional del Sur & IFISUR (UNS-CONICET), Av. Alem 1253, (8000) Bahía Blanca, Argentina

ARTICLE INFO

Article history:
Received 16 November 2010
Received in revised form
31 March 2011
Accepted 12 April 2011
Available online 24 May 2011

Keywords:
Hydrogen adsorption
Platinum
Co-adsorption
Surface energy

ABSTRACT

In this work, we present a density functional theory (DFT) study of hydrogen interaction with Pt on a B2 FeTi (110) metallic surface. DFT is used to trace relevant orbital interactions and to discuss the electronic consequences of incorporating H on Fe–Ti bonding. We determined the optimal location for Pt and, then, for adsorbed hydrogen. In addition, we followed the density of states and changes in chemical bonding both in the surface and the adsorbates. The overlap population analysis reveals metal–metal bond breaking after hydrogen adsorption, thus being the inter-metallic bond the most affected one.

1. Introduction

Hydrogen storage is an important topic today in the search for a clean, renewable, and sustainable type of energy. In contrast to fossil fuels, hydrogen does not produce any type of pollution that could increase the greenhouse effect; even more, when it is used in fuel cells, the final product -besides electricity- is water [1].

On the other hand, the H–metal interaction is a very important area due to the influence of hydrogen on metallic, mechanical, and electrical properties. The study of the H–metal interaction is also important to understand the process that takes place in embrittlement and corrosion of metals and alloys [2,3,4,5,6,7]. In order to measure the hydrogenation and how good the compounds are for storage, different techniques could be found, such as those used by Jain et al. [8] and Busch et al. [9] where a neutron diffraction and a by using Elastic Recoil Detection Analysis with Ag107 ions. These two techniques have shown good results in detecting the hydrogenation level in different alloys suck as magnesium and FeTi compounds.

Several criteria need to be considered when a material is studied for hydrogen storage. Bououdina et al. [10] described the requirements for an optimum storage: *i)* high storage capacity, *ii)* low dissociation temperature, *iii)* medium pressure for dissociation, *iv)* low formation energy, *v)* low production cost, *vi)* low weight -therefore, it is transportable, *vii)* stability in the presence of O_2. Sakar & Banerjee [11] have done a comparison among different ways of hydrogen storage for vehicle purposes, the FeTi hydrides is not the best but is one of the best and therefore its relevance for the works on hydrogen storage as energy vector.

The inter-metallic compound FeTi is a very attractive compound meeting these requirements, cheap, and with

* *Corresponding author*. Chemical Engineering Department, Faculty of Natural Science and Technology, Sem Sælands v. 4, 7491 Trondheim, Norway. Tel.: +54 291 4595101x2800–2818; fax: +54 291 4595142.
E-mail address: jorge.marchetti@chemeng.ntnu.no (J.M. Marchetti).
0360-3199/$ – see front matter
doi:10.1016/j.ijhydene.2011.04.085

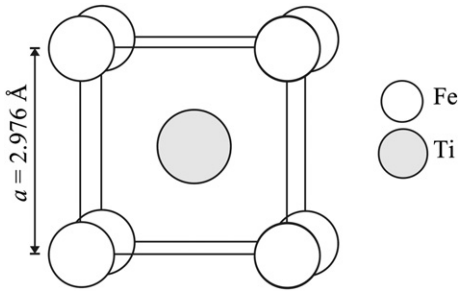

Fig. 1 – Unit cell of the B2 FeTi alloy.

a storage capacity of 1.9%. When hydrogen interacts with FeTi, two possible phases are formed, $FeTiH_{\sim 1}$ (β-phase) and $FeTiH_{\sim 2}$ (γ-phase) [12]:

$$2.13FeTiH_{0.1}(\alpha) + 1.001H_2 \rightarrow 2.13FeTiH_{1.04}(\beta) \quad (1)$$

$$2.20FeTiH_{1.04}(\beta) + 0.932H_2 \rightarrow 2.13FeTiH_{1.95}(\gamma) \quad (2)$$

Several works have shown that FeTi is an excellent hydrogen storage material due to the formation of hydrides [13,14,15,16,17,18,19]. The addition of other metals to the surface of this alloy improves its storage capabilities. In an effort to understand these improvements, Kim et al. [20] studied the effect of the addition of Pd on a B2 FeTi alloy. These authors have found that metal–hydrogen interaction increases when Pd is in contact with both Fe and Ti. The presence of Pd increases the speed of this process on a Pd/FeTi (100) surface. Bououdina et al. [21] have also considered Ni instead of Pd. The presence of Ni in this material improves the kinetics of adsorption. On the other hand, Pt could be potentially useful to improve the adsorptive properties of FeTi intermetallic surface [20]. In addition, platinum is well known for its catalytic properties and its widespread use in gas convertors as well as fuel cell electrodes [22,23,24,25,26].

In this work, we present a study of hydrogen interaction with platinum on B2 FeTi (110) metallic surface. We have determined H and Pt in their energy minimal locations and we have also followed the density of states and bonding changes both in the surface and with adsorbates.

2. Surface model and computational method

The inter-metallic B2 FeTi structure is a BCC with a lattice parameter of $a = 2.976$ Å [14]. We selected the (110) crystallographic plane and used a vacuum region of three–lattice parameters in order to avoid the interaction between surfaces. Fig. 1 shows the unit cell. Density Functional Theory (DFT) is used to compute adsorption energies, trace relevant orbital interactions and to discuss the electronic consequences of incorporating H on Fe–Ti bonding. In the next sections, we consider the theory and the adsorption models.

2.1. *Computational method*

Generalized gradient approximation density functional theory (GGA-DFT) calculations were performed on a super cell containing 122 atoms (72 Fe and 50 Ti) in a cubic lattice (B2-phase). Lattice parameters were determined by minimizing the total energy of the cell using a conjugated-gradient algorithm to relax the ions [27]. A $4 \times 4 \times 4$ Monkhorst-Pack k-point grid for sampling the Brillouin zone was considered. No significant change in energy was observed performing calculations with larger sets of k-points. For this, we used the Amsterdam

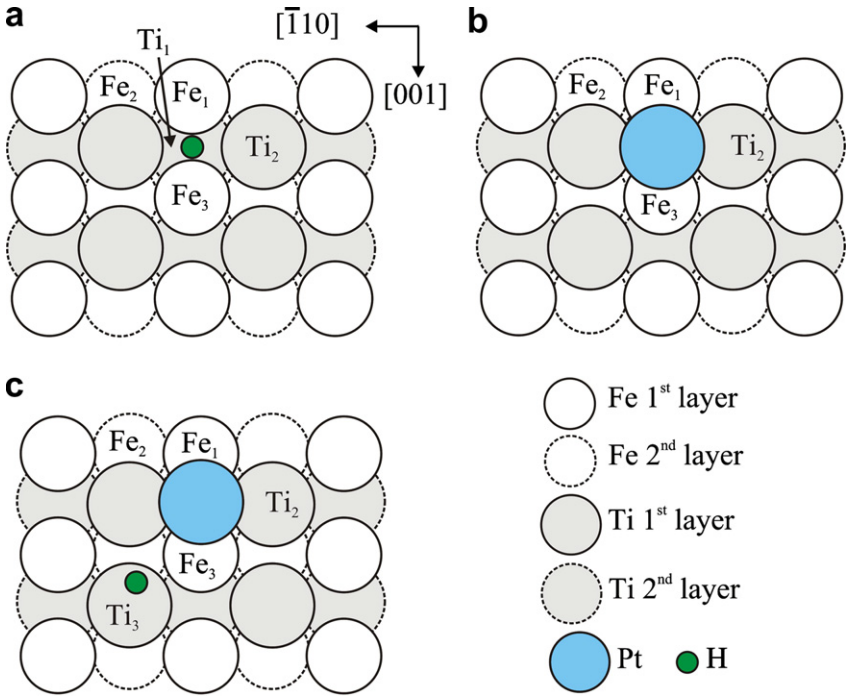

Fig. 2 – Schematic top view of the B2 FeTi(110) surface slab. (a) H, (b) Pt and (c) H and Pt co-adsorbed minimum position.

Table 1 – Electronic Orbital Occupation, OP and distances on FeTi (110) clean H and Pt cover surface.

Structure	Electronic occupation			Bond	OP	ΔOP%[c]	Distance (Å)
	s	p	d	Type			
FeTi							
Fe_1	0.81	0.04	8.57	Fe_1–Fe_3	0.198	–	2.976
Ti_1	0.45	0.12	1.05	Ti_1–Ti_2	0.024	–	2.976
				Fe_1–Ti_2	0.285	–	2.577
FeTi + H[a]							
Fe_1	0.58	0.09	8.09	Fe_1–Fe_3	0.067	−66.2	2.976
Ti_1	0.41	0.08	0.89	Ti_1–Ti_2	0.005	−79.2	2.976
Ti_2	0.38	0.10	0.80	Fe_1–Ti_2	0.213	−25.3	2.577
H	1.29	0.00	0.00	H–Fe_1	0.406		1.491
				H–Ti_1	0.031		2.004
				H–Ti_2	0.022		2.111
FeTi + Pt[b]							
Fe_1	0.73	0.22	6.45	Fe_1–Fe_3	0.041	−79.3	2.976
Ti_1	0.43	0.09	1.04	Ti_1–Ti_2	0.000	−100	2.976
Ti_2	0.44	0.17	1.03	Fe_1–Ti_2	0.135	−52.6	2.577
Pt	1.28	2.76	8.93	Pt–Fe_1	1.315		1.849
				Pt–Ti_1	0.034		3.137
				Pt–Ti_2	0.802		1.930

a $\Delta E_F = 0.03$ (adsorbed hydrogen).
b $\Delta E_F \approx 0$ (adsorbed platinum).
c Percentages are related to clean surface.

Density Functional package (ADF-DFT) [28]. Further details of the calculations are given in [29,30].

2.2. *Surface and adsorption model*

We used the super cell technique to represent the (110) plane. In order to achieve the best compromise between computational time and accuracy of our model, we decided to use a seven layer-slab separated in the [001]-direction by vacuum regions. The thickness of the vacuum region, corresponding to 12 Å, was enough to avoid interaction of the atoms on the surfaces. The thickness of B2 FeTi(110) slab should be such that it approaches the electronic structure of 3D bulk FeTi in its innermost layer. The interlayer spacing in this FeTi(110) model is 2.104 Å. Our slab has two identical surface-like layers and five inner layers. Fig. 2 shows the first two layers of the slab.

For H adsorption on the FeTi(110) surface, a very low coverage model was considered. The (110) surface has six different high-symmetry adsorption sites: on top of a substrate atom (Fe-top and Ti-top), in a position that forms a bridge (B) between two nearest-neighbor surface atoms (the Fe–B and Ti–B positions) and in two four-fold hollow locations (see Fig. 2a). The distances between the adsorbed H atom and the Fe or Ti subsurface atoms are 1.83 Å for the top position and 1.17 Å for the bridge position. The H-surface distance was optimized considering relaxation for the first two layers of the metal slab. Additional H adsorption calculations were performed considering the pre-adsorption of a single Pt atom on the FeTi surface. Pt is considered and ad-atom that can change the local

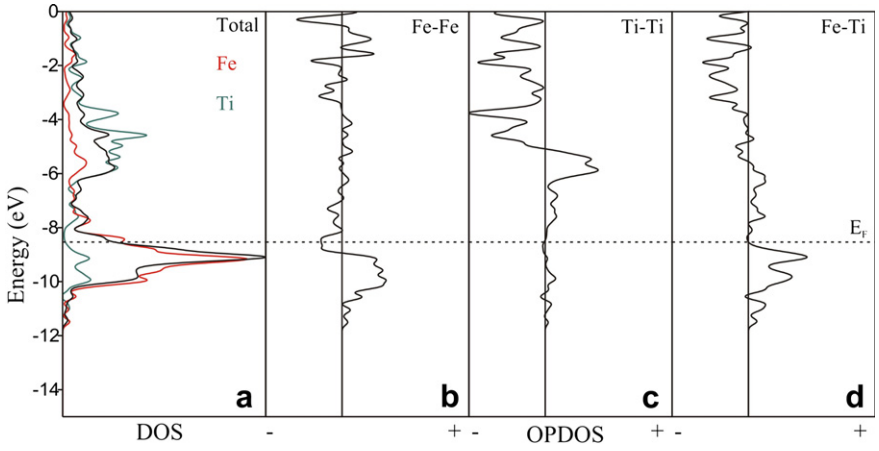

Fig. 3 – DOS curves for FeTi(110) before impurity adsorption. (a) Total, DOS projected on a Fe atom (red line) and on a Ti atom (green line). OPDOS curves for FeTi(110) before impurity adsorption: (b) Fe–Fe, (c) Ti–Ti and (d) Fe–Ti bonds. (For interpretation of the references to colour in this figure legend, the reader is referred to the web version of this article.)

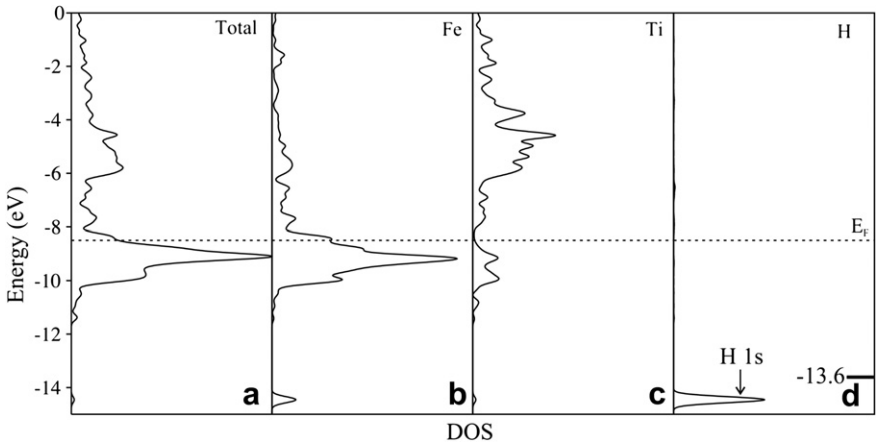

Fig. 4 – DOS curves for the B2 FeTi(110) with Hydrogen adsorbed. (a) Total, (b) DOS projected on a Fe atom, (c) on a Ti atom and (d) on H atom.

environment for H. We started our calculations with Pt located in the high-symmetry adsorption sites and then allowed to relax.

3. Results and discussion

As the first step in our calculations we computed the electronic structure of the clean FeTi (110) surface. Table 1 present the electron orbital occupation for both Fe and Ti and also the overlap population (OP). It is important to mention that Ti–Ti is weaker than Fe–Fe or Fe–Ti interactions. Fig. 3.a shows the DOS curves for the clean slab. It can be seen that the d band that goes from −12 to −8 eV corresponds to iron contributions and from −8 to −3 eV it corresponds to Ti. The d band is filled. These results are in agreement with those obtained by Papaponstantopoulos [31], where the iron contribution is below Fermi level, while titanium is above it. The OPDOS for the clean FeTi surface is presented in Fig. 3b, c, and d. The curves present more bonding contributions for Fe–Fe and Fe–Ti bonds and we can see some antibonding states in the case of Fe–Fe bond [30]. Our results are in agreement with those obtained by Kinaci & Aydinol [1], who reported that iron only participates in the antibonding region when the crystal structure is orthorhombic.

3.1. *The adsorption of hydrogen and platinum*

Hydrogen and platinum were first adsorbed separately on the slab in order to explain the effects of a very active transition metal. Lee et al. published detailed local density approximations (LDA) calculations for clean and H adsorbed B2 TiFe surfaces [15]. In this work, the authors use a seven layer-slab and the hydrogen adsorption was studied only on hollow sites in the case of (110) plane, considered more stable in many metals surfaces.

Fig. 2a shows the final geometry for H on the clean surface. The four-fold hollow location, closer to Fe atoms (Fe_1 and Fe_3), is 0.24 eV more stable than the top or bridge sites and the H-surface distance is −0.10 Å. The computed adsorption energy is 0.87 eV which is an intermediate value when compared with Fe or Ti terminated surfaces [15]. The H–Fe distance is close to that reported on Fe (110) by Juan & Hoffman [32] and the H–Ti distance is in agreement with the one reported by Moritz et al. [33]. From Table 1, it can be seen, that the distances between hydrogen and Fe and Ti are 1.491 and 2.001 Å, respectively. These values are also close to that reported by Lee et al. [15], (1.8 Å for the top position). A similar work done by Jasen et al. [34] studying the interaction of H with a FePd slab, reported that the distance between H and Fe is about 1.337 Å. The difference between

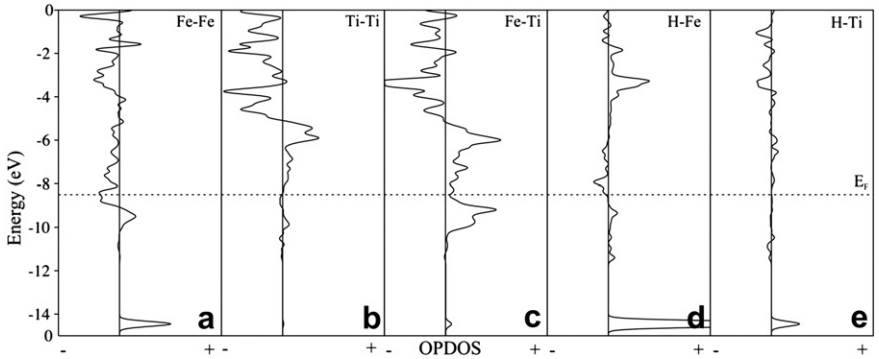

Fig. 5 – OPDOS curves for the B2 FeTi(110) after H adsorption. (a) Fe–Fe, (b) Ti–Ti, (c) Fe–Ti, (d) H–Fe and (e) H–Ti bonds.

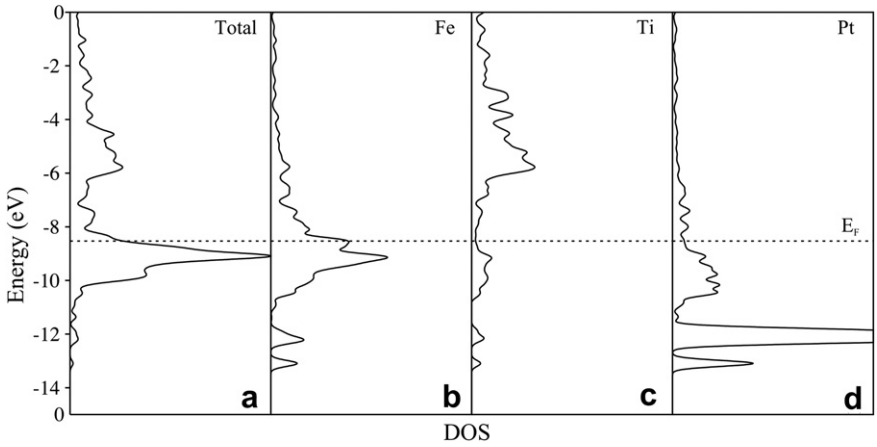

Fig. 6 – DOS curves for the B2 FeTi(110) after Pt adsorption. (a) Total, (b) DOS projected on a Fe atom, (c) on a Ti atom and (d) on Pt atom.

these two values is due to the different component in the alloy used.

H introduces important changes in the electronic structure of the surface. The changes come from a bond formation after hybridization between H1s state and s and d states from Ti and Fe. The overlap population values in Table 1 decrease for all metal–metal bonds, being the more affected Ti_1–Ti_2, while metal–H bonds develop. Fig. 4 shows the DOS plots after hydrogen adsorption. A small peak at −14 eV is due to the projection of H1s orbital, this peak is higher in the Fe projection (Fig. 4b). The OPDOS plots in Fig. 5 show a more developed antibonding region for Ti–Ti bond if we compare Fig. 5.b with Fig. 3.c close to E_f. This effect is attributed to H and was also reported by Kinaci and Aydinol [1]. H–Ti and H–Fe interactions are both bonding with a peak near −14 eV, which also serves as bonding for the metal–metal bond. However, the Fe–Fe OPDOS area is smaller, a clear indication of metal–metal bond weakening.

Pt is adsorbed bridging two Fe and two Ti atoms (see Fig. 2b) at a distance from the surface of 1.01 Å. The Pt–Fe bond is shorter than the Pt–Ti and the location is above a four-fold hollow. The adsorption energy and geometry indicates a strong Pt-surface interaction close to that reported by Lee et al. in the case of Pd/FeTi [15]. Table 1 shows that the s band of the slab is partially filled, 1/3 for Fe and 1/5 for Ti. The important decrease in the metal–metal OP indicates that the strong Pt–Fe bond is developed at expenses of all the other metal–metal bonds. Fig. 6 shows the changes in the DOS plot when Pt is adsorbed. Its presence does not change the total density of states considerably, where the main contribution is due to Fe or Ti. There are new peaks with energies lower than −12 eV due to Pt. Fig. 7 shows the OPDOS for the same system. It can be seen that Pt–Ti, Pt–Fe, and Fe–Ti interactions are mainly bonding. If we compare these plots with those for the metal–metal OPDOS before adsorption (Fig. 3 b–d) we can see that bonding area decrease while the Pt–Fe and Pt–Ti bonding interaction increase (see Fig. 7 d and e). This effect was also reported in the literature [34,35] for different metal systems.

3.2. *The co-adsorption of hydrogen and platinum*

After considering both impurities separately, we shall now consider the combined effect of Pt and Hydrogen co-adsorption. Lee et al. [15] studied the adsorption of hydrogen on a slab of TiFe(110) with a Palladium monolayer on the surface. These authors have found that the hydrogen atom was adsorbed between the Pd layer and the TiFe surface using LDA-DFT approximation. In the present study, we used a single Pt atom in order to shed light on the metal–hydrogen

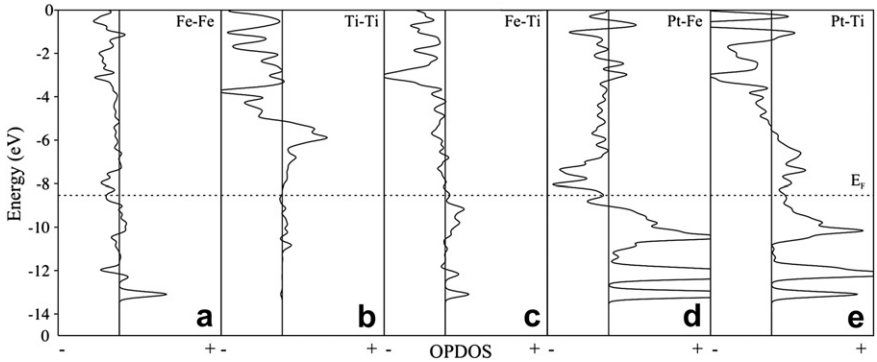

Fig. 7 – OPDOS curves for the B2 FeTi(110) after Pt adsorption. (a) Fe–Fe, (b) Ti–Ti, (c) Fe–Ti, (d) Pt–Fe and (e) Pt–Ti bonds.

Table 2 – Electronic Orbital Occupation, OP and distance on FeTi (110) surface when Pt is fixed and Hydrogen is adsorbed.

Structure	Electronic occupation			Bond	OP	ΔOP%[a]	Distance (Å)
	s	p	d	Type			
(FeTi + Pt) + H							
Fe_1	0.73	0.22	6.42	Fe_1–Fe_3	0.043	4.87	2.976
Ti_1	0.43	0.08	1.04	Ti_1–Ti_2	0.001	0	2.976
Ti_2	0.44	0.17	1.03	Fe_1–Ti_2	0.134	−0.74	2.577
Pt	1.28	2.74	8.92	Pt–Fe_1	1.316	0.08	1.849
				Pt–Ti_1	0.035	2.94	3.137
				Pt–Ti_2	0.800	−0.25	1.930
Fe_3	0.71	0.35	6.13				
H	1.49	0.00	0.00	H–Pt	0.000	–	3.253
				H–Fe_3	0.077	–	2.275
Ti_3	0.41	0.25	0.97	H–Ti_3	0.570	–	1.253

a OP percentages are related to the surface with adsorbed Pt.

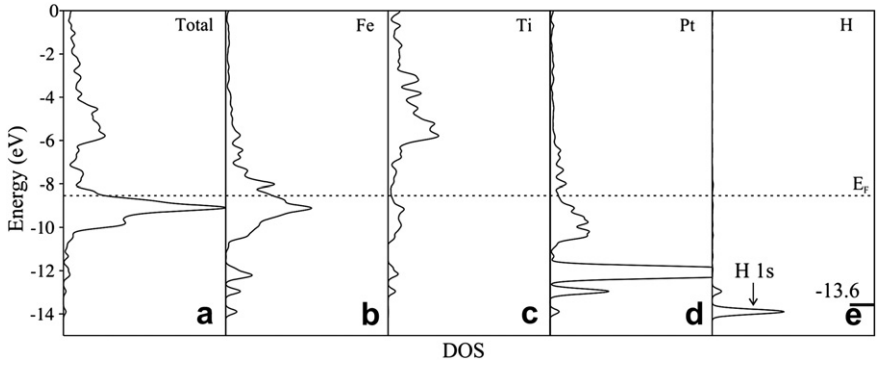

Fig. 8 – DOS curves for the B2 FeTi(110) with Pt atom fixed location and after H adsorption. (a) Total, (b) DOS projected on a Fe atom, (c) on a Ti atom, (d) on Pt atom and (e) on H atom.

bond effect. Fig. 2c shows a top view of the slab with the adsorption of both atoms, Pt and H. The presence of Pt changes the preferential site for H adsorption, being top on a neighbor Ti atom with and adsorption energy of 0.97 eV that is 0.10 eV more stable than the clean FeTi surface. Pt also produced a change in the ΔOP (compare Table 1 with Table 2), reducing the detrimental effect of H on the metal–metal bonds because only Ti_3 is affected. Changes in the DOS as well as OPDOS plots provide some additional information. The presence of the hydrogen atom produces a small modification on the electronic structure of the slab; in particular, the bands for the Fe atom are slightly changed. A similar effect can be seen on the Ti atoms due to the presence of Pt. Fig. 8 shows that the bands below the Fermi level come from Fe atoms, while at higher energies they correspond to Ti. The peak at −14 eV belongs to H 1s stabilized orbital, while the peak at −12 eV, the band between −11 eV and the Fermi level all belong to Pt. The peak at −13 eV is also present in the H projected DOS revealing some weak H–Pt interaction (see Fig. 8d). OPDOS curves are shown in Fig. 9; all the bonds have a main bonding area that is higher for Pt–Fe and Pt–Ti bonds. H–Fe and H–Ti peaks are noticeable at −14 eV, being completely

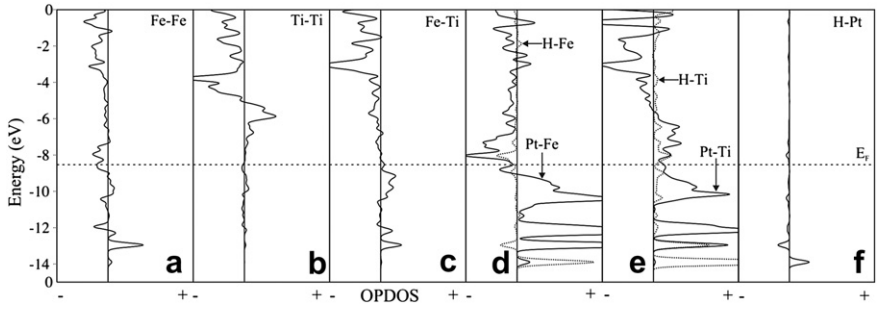

Fig. 9 – OPDOS curves for the B2 FeTi(110) with Pt atom fixed position and after H adsorption. (a) Fe–Fe (a), (b) Ti–Ti, (c) Fe–Ti, (d) H–Fe and Pt–Fe, (e) H–Ti and Pt–Ti and (f) H–Pt bonds.

bonding toward Ti. In the case of the H–Fe bond, there is a slightly antibonding region -see Fig. 9d; in the case of the H–Pt bond it can be seen that the interaction is non- bonding because bonding and antibonding almost compensate. The OP value for the H–Pt bond in Table 2 is zero, in accordance with the compensation effect shown in Fig. 9f. In addition, the decrease in the Fe–Fe and Ti–Ti OP is due to the increase of Pt–Ti and Pt–Fe bond strengthening and the formation of new Ti–H and Fe–H bonds.

4. Conclusions

Our results indicate that, in the clean surface, hydrogen is located on a hollow site interacting with both two Fe and Ti atoms and going below the surface. On the other hand, Pt locates in a hollow position above the surface connecting Fe's and Ti's. The H–Fe distance is close to the one reported on Fe (110) by Juan & Hoffman [32] and the H–Ti distance is in agreement with the one reported by Moritz et al. [33]. For the clean FeTi surface, few antibonding states are observed for the Fe–Fe bond in agreement with those reported by Kinaci & Aydinol [1]. H–Ti and H–Fe interactions are both bonding. However, the area of the Fe–Fe OPDOS is smaller, thus indicating bond weakening. When Pt is adsorbed, the Fe–Fe bond is also weakened and a Pt–Fe bond is formed at the expense of iron bonds. The DOS and OP values indicate a strong Pt-surface interaction close to that reported in the literature. In the case of H and Pt co-adsorption, Pt creates a bond that is 12% more stable in energy for the metal–H interaction. H location changes and becomes closer to Ti atoms with an H–metal distance of 1.253 Å. The OPDOS curves show that all the bonds have a main bonding area, being higher for Pt–Fe and Pt–Ti bonds. H–Fe and H–Ti peaks are noticeable at −14 eV, being completely bonding toward Ti.

Acknowledgments

Our work was supported by PICT 1770, PICT-PRH 2011, PIP-CONICET 2009, and PGI-SGCyT-UNS. JMM would like to thank NTNU in Norway for allowing him to carry out this collaboration work. All the authors are members of CONICET (Argentine Commission for Scientific and Technical Research). We also thank the useful reviewer's comments.

REFERENCES

[1] Kinaci A, Aydinol MK. Ab initio investigation on FeTi–H system. Int J Hydrogen Energy 2007;32:2466–74.
[2] Chêne J, Brass AM. Hydrogen transport by mobile dislocations in nickel base super alloy single crystals. Scripta Mater 1999;40(5):537–42.
[3] Brass AM, Chêne J. Hydrogen adsorption in titanium aluminides exposed to aqueous solutions at room temperature. Mater Sci Eng A 1999;272(2):269–78.
[4] Brass AM, Chêne J. Influence of deformation on the hydrogen behavior in iron and nickel base alloys: a review of experimental data. Mater Sci Eng A 1999;242(1–2):210–21.
[5] Krom A, Koers R, Bakker A. Hydrogen transport near a blunting crack tip. J Mech Phys Solids 1999;47(4):971–92.
[6] Hirth JP, Carnahan B. Hydrogen adsorption at dislocations and cracks in Fe. Acta Metall 1978;26:1795–803.
[7] Kummick AJ, Johnson HH. Deep trapping states for hydrogen in deformed iron. Acta Metall 1981;28:33–9.
[8] Jain IP, Devi B, Sharma P, Williamson A, Vijay YK, Avasthi DK, et al. Hydrogen in FeTi thin films by ERDA with Ag^{107} ions. Int J Hydrogen Energy 2000;25:517–21.
[9] Busch G, Schlapbach L, Stucki F, Fischer P, Andresen AF. Hydrogen storage in FeTi: surface segregation and its catalytic effect on hydrogenation and structural studies by means of neutron diffraction. Int J Hydrogen Energy 1979; 4:29–39.
[10] Bououdina M, Grant D, Walker G. Review on hydrogen adsorbing materials-Structure, microstructure, and thermodynamics properties. Int J Hydrogen Energy 2006; 31(2):177–82.
[11] Sarkar A, Banerjee R. Net energy analysis of hydrogen storage options. Int J Hydrogen Energy 2005;30:867–77.
[12] Reilly JJ, Wiswall RH. Formation and properties of iron titanium hydrides. Inorg Chem 1974;13(1):218–22.
[13] Saita I, Sato M, Uesugi H, Akiyama T. Hydriding combustion synthesis of TiFe. J Alloys Comp 2007;446–447:195–9.
[14] Villars P, Calvert LD. Pearson's Handbook of crystallographic data for intermetallic phases. Metals Park, OH: American Society for Metals; 1985.
[15] Lee G, Kim JS, Koo YM, Kulkova SE. The adsorption of hydrogen on B2 FeTi surfaces. Int J Hydrogen Energy 2002; 27(4):403–12.
[16] Schober T, Westlake DG. The activation of FeTi for hydrogen storage: a different view. Scripta Metall 1981;15(8):913–8.
[17] Schober T. On the activation of FeTi for hydrogen storage. J Less Comm Metals 1983;89(1):63–70.
[18] Kim HC, Lee JY. The effect of surface conditions on the activation of FeTi. J Less Comm Metals 1985;105(2):247–53.
[19] Kim HC, Lee JY. A study on the activation mechanism of FeTi in view of surface conditions of metals. Int J Hydrogen Energy 1985;10(7/8):543–5.
[20] Kim JS, Oh SY, Lee G, Koo YM, Kukova SE, Egorushkin VE. Theoretical study of the electronic structure and hydrogen adsorption properties in B2 FeTi thin films with Pd coating. Int J Hydrogen Energy 2004;29(1):87–92.
[21] Bououdina M, Fruchart D, Jacquet S, Pontonnier L, Soubeyroux JL. Effect of nickel alloying by using ball milling on the hydrogen absorption properties of TiFe. Int J Hydrogen Energy 1999;24(9):885–90.
[22] Ford DC, Xu Y, Mavrikakis M. Atomic and molecular adsorption on Pt(111). Surf Sci 2005;587(3):159–74.
[23] Eichler A, Hafner J. Reaction channels for the catalytic oxidation of CO on Pt(111). Phys Rev B 1999;59(8):5960–7.
[24] Cortright RD, Davda RR, Dumesic JA. Hydrogen from catalytic reforming of biomass-derived hydrocarbons in liquid water. Nature 2002;418(6901):964–7.
[25] Dunn S. Hydrogen future: towards a sustainable energy system. Int J Hydrogen Energy 2002;27(3):235–64.
[26] Barreto L, Makihira A, Riahi K. The hydrogen economy in the 21st century: a sustainable development scenario. Int J Hydrogen Energy 2003;28(3):267–84.
[27] Press WH, Flannery BP, Teukolsky SA, Vetterling WT. Numerical Recipies. New York: Cambridge University Press; 1986.
[28] Amsterdam density functional package release. Amsterdam: Vrije Universiteit; 2001.
[29] González EA, Jasen PV, Brizuela G, Juan A, Nieminen R. The effect of interstitial hydrogen on the electronic

structure of the B2 FeAl alloy. Phys Status Solidi B 2007; 244(10):3684–94.
[30] Hoffmann R. Solids and surfaces: a chemist's view of bonding in extended structures. New York: VCH; 1988.
[31] Papaponstantopoulus DA. Handbook of band structures of elemental solids. New York: Plenum Press; 1986.
[32] Juan A, Hoffmann R. Hydrogen on the Fe(110) surface and near bulk bcc Fe vacancies: a comparative bonding study. Surf Sci 1999;421(1–2):1–16.
[33] Moritz W, Imbihl R, Behm RJ, Ertl G, Matsushima T. Adsorption geometry of hydrogen on Fe(110). J Chem Phys 1985;83(4):1959–68.
[34] Jasen PV, Gonzalez EA, Castellani NJ, Juan A. Theoretical study of hydrogen adsoprtion on FePd face centered cubic alloy surface. Phys Rev B 2005;71(23):1–7.
[35] Marchetti JM, Gonzalez EA, Jasen PV, Brizuela GP, Juan A. Hydrogen adsorption and diffusion on a Pt(111) cluster. Surf Rev Let 2008;15(3):319–27.